

DOI: 10.1002/((please add manuscript number))

**Article type: Communication**

## **Surface crystallization of liquid Au-Si and its impact on catalysis**

*Federico Panciera,\* Jerry Tersoff, Andrew D. Gamalski, Mark C. Reuter, Dmitri Zakharov, Eric A. Stach, Stephan Hofmann, Frances M. Ross\**

Dr. F. Panciera, Prof. S. Hofmann

Department of Engineering, University of Cambridge, 9 J. J. Thomson Avenue, Cambridge CB3 0FA, UK

Dr. F. Panciera

Current address: Centre de Nanosciences et de Nanotechnologies, CNRS, Université Paris-Sud, Université Paris-Saclay, Avenue de la Vauve, 91120 Palaiseau, France.

E-mail: federico.panciera@c2n.upsaclay.fr

Dr. F. Panciera, Dr. J. Tersoff, Dr. M. C. Reuter, Dr. F. M. Ross

IBM T. J. Watson Research Center, Yorktown Heights, NY 10598, USA

E-mail: fmross@mit.edu

Dr. A. D. Gamalski, Dr. D. Zakharov, Dr. E. A. Stach

Center for Functional Nanomaterials, Brookhaven National Laboratory, Upton, NY 11973, USA

Dr. F. M. Ross

Current address: Department of Materials Science and Engineering, Massachusetts Institute of Technology, 77 Massachusetts Avenue, Cambridge, MA 02139, USA

Keywords: (surface freezing, nanowires, *in situ* transmission electron microscopy, 2D crystals, metastable phases)

### **Abstract:**

In situ transmission electron microscopy reveals that an atomically thin crystalline phase at the surface of liquid Au-Si is stable over an unexpectedly wide range of conditions. By measuring the surface structure as a function of droplet temperature and composition, a simple thermodynamic model is developed to explain the stability of the ordered phase. The results show that the presence of surface ordering plays a key role in the pathway by which the Au-Si eutectic solidifies, and also dramatically affects the catalytic properties of the liquid, explaining the anomalously slow growth kinetics of Si nanowires at low temperature. A strategy to control the presence of the surface phase is discussed, using it as a tool in designing strategies for nanostructure growth.

**Text:**

Understanding the phenomena that occur at the surface of liquid metals is critical for technological applications ranging from catalysis to soldering to crystal growth. However, liquid metal surfaces can be complex and exhibit puzzling phenomena. Liquid metal alloys commonly exhibit Gibbs adsorption effects, where the surface layer is enriched in the element with the lower surface tension<sup>[1,2]</sup>. Density oscillations are also commonly observed at the surface,<sup>[3,4]</sup> and even surface ordering.<sup>[1,2,5,6,7]</sup> Au-Si, a liquid metal, is unique in forming a two-dimensional (2D) crystalline compound at its surface, with a fixed atomic-scale thickness, over a range of temperature. While this layer has not been imaged directly, diffraction studies have established that an ordered bilayer (the “LT phase”) exists up to 12 °C above the eutectic temperature.<sup>[2,8]</sup> (A higher-temperature phase has also been detected, although its properties are less clear.<sup>[9,10]</sup>) At present there is no clear explanation for this unique behaviour. Ordered surface phases have been explained by surface pre-freezing,<sup>[11]</sup> a phenomenon that is analogous to the well-known surface pre-melting. However, an ordered pre-freezing layer is expected to be present only very near the transition temperature and to have a thickness that diverges as the temperature approaches the transition temperature, both of which are inconsistent with the behavior of Au-Si. The ordered surface phase in Au-Si also cannot be explained as a solute coming out of solution and wetting the surface, as can occur in dilute Ga solutions.<sup>[6]</sup>

Here, we use *in situ* transmission electron microscopy (TEM) to observe directly the formation of a crystalline 2D compound at the surface of liquid Au-Si. By varying both temperature and composition we find that the 2D phase can be stable over a surprisingly large range, over 150 °C, extending above and below the eutectic temperature. We develop a simple thermodynamic model that explains the wide stability range and composition dependence. Given the persistence of the surface ordering, we explore its effects on critical aspects of the behaviour of Au-Si. We find that the surface layer plays a key role in the pathway of eutectic

decomposition of Au-Si into solid Au + solid Si on cooling, and also that it is the root cause of the dramatic changes observed in the catalytic properties on cooling. We derive a strategy for controlling the presence of the surface phase as a tool in nanostructure fabrication.

Surface ordering on droplets of Au-Si of different diameters is shown in **Figures 1a, 1b** and Movie S1. This high spatial and temporal resolution data (see Supporting Information) was recorded by *in situ* heating of Si substrates decorated with Au nanoparticles, optionally while exposed to the Si source gas disilane ( $\text{Si}_2\text{H}_6$ ). On reaching the Au-Si eutectic temperature  $T_E = 363\text{ }^\circ\text{C}$ ,<sup>[12]</sup> the Au reacts with Si to form Au-Si liquid droplets. Imaging the surfaces of these droplets in profile view (Figure 1a) shows that there are two well-defined crystalline layers at the surface. The ordering can also be detected in projection over the entire droplet area in Figure 1a. In the smaller droplet shown in Figure 1b, bending rigidity of the surface phase is evident: the droplet is deformed into a polyhedron bounded by relatively flat “facets”, having radius of curvature 80-100 nm, that meet at higher angle edges. The facets and edges undergo dynamic motion at the measurement temperature, shown in Movie S1. To eliminate effects of surface oxidation or other extraneous reactions that may arise from the microscope background vacuum (relatively poor at  $10^{-6}$  Torr), identical experiments were carried out in a TEM with an ultra-high vacuum sample environment ( $2 \times 10^{-10}$  Torr). In this instrument, we identify surface ordering under equivalent conditions via the faceting of otherwise liquid droplets, even though the atomic level details at the surface are not resolved.

We evaluate the presence and structure of the surface phase as a function of temperature by heating and cooling droplets on a Si substrate. A cooling and reheating cycle is shown schematically in Figure 1c. The droplet exhibits supercooling, remaining in a liquid state well below  $T_E$ ; at  $\sim 250\text{ }^\circ\text{C}$  Au and Si rapidly separate and solidify; then liquid reappears as  $T_E$  is reached. The surface ordering shows distinctive behaviour. On cooling, it consistently appears at  $\sim 370\text{ }^\circ\text{C}$  and remains visible until solidification. On heating, it becomes visible as soon as

liquid starts to appear at  $T_E$  (Figure 1d) and it persists up to 410 °C. The pronounced temperature hysteresis suggests a first order phase transition at 410 °C, with supercooling to 370 °C before the ordered phase appears.

A striking feature of the ordered surface layer in Figure 1c is that its structure and thickness appear constant over its range of stability, with no other phase visible. We also find that a structure with similar lattice parameters is present on the surface of solid Au at temperatures where ordering is present on the liquid (Figure 1d, with more detail in Figure S1). The lattice spacing, number of crystalline layers and stiffness of the ordered surface layer correspond to the LT surface phase previously identified<sup>[2]</sup> in diffraction (Table S1), and the bending rigidity is also consistent with the LT phase.<sup>[8,2]</sup> However, in our experiments the surface ordering is stable up to 410 °C, much higher than the stability up to 371 °C reported for LT.<sup>[2]</sup>

To understand the driving force that forms the surface ordering, and its unexpected stability, we first note, as above, that our system is not exhibiting classic pre-freezing,<sup>[11]</sup> since the surface phase does not change its thickness even over a range of 150 °C. On the other hand, its formation can not be explained using bulk thermodynamic arguments since Au-Si solid compounds are not present on the phase diagram. To develop a model that explains the observations we therefore probe in more detail the conditions under which the surface phase is stable on liquid Au-Si, addressing its dependence on both composition and temperature.

We first explore the formation of the surface phase as a function of composition, Figure 2a. This was achieved by placing Au nanocrystals on an inert support (see Experimental Section), heating to a fixed temperature, then gradually adding Si by flowing the source gas disilane ( $\text{Si}_2\text{H}_6$ ). As expected from the phase diagram,<sup>[12]</sup> above  $T_E$  the Au is progressively converted to Au-Si liquid. Further addition of Si enriches the liquid in Si, eventually nucleating solid Si (Movie S2). During this sequence, the presence of surface ordering can be evaluated. At 410 °C, surface ordering is not present on the Au-Si when it forms initially, but appears as

the Au-Si composition approaches the Si liquidus line (i.e. shortly before Si nucleation). At lower temperatures, surface ordering becomes visible closer to the Au liquidus line (Figure S2). At 370 °C or below, surface ordering is visible as soon as any liquid forms, i.e. at the Au liquidus composition. This is shown on the phase diagram in Figure 2C. The transition temperature between ordered and disordered surfaces increases sharply with Si composition. To evaluate the stability of surface ordering as a function of temperature, we examine Au-Si droplets that are in contact with Si, Figure 2b. As the temperature varies, the presence of the Si reservoir fixes the Au-Si at the liquidus composition. Ordering is visible between  $T_E$  and 410 °C. This stability range is consistent with Figure 1B and is shown as a triangle on the phase diagram in Figure 2c.

To model the phase boundary between the ordered and disordered liquid surface, we consider the 2D surface phase to be a surface reconstruction of the liquid. We then calculate the transition as we would the transition between two reconstructions of a solid surface, via minimization of the surface free energy. We assume that the structure and composition of the 2D solid are fixed, and correspond to that reported for the LT phase ( $\text{Au}_4\text{Si}_8$ ).<sup>[2]</sup> For simplicity we neglect all non-essential effects, including finite size effects as well as any variation of the liquid-vapor and liquid-solid interfacial free energies or of the net interfacial segregation in the liquid with composition and temperature. With these approximations, we can write the free energy change  $\Delta F_s$  upon forming an ordered surface layer as

$$\Delta F_s = \Delta \Gamma_s - N_{Au} \mu_{Au} - N_{Si} \mu_{Si} \quad \text{Equation 1}$$

where the solid has areal density  $N_{Au}$  and  $N_{Si}$  of Au and Si atoms, respectively, and the  $\mu$ 's are the chemical potentials of these atoms in the liquid. It is convenient to take elemental solid Au and Si as reference states, so  $\Delta \Gamma_s$  is the change in free energy upon taking  $N_{Au} + N_{Si}$  atoms from the reference solids and assembling them as a 2D crystal on the liquid surface. Since the surface phase corresponds well with the LT phase, we use the  $N$  values given in Ref. 2 and  $\mu_{Au}$

and  $\mu_{Si}$  are calculated using a standard thermodynamic model.<sup>[13]</sup> We neglect the entropic component of  $\Delta\Gamma_s$ , treating  $\Delta\Gamma_s$  as independent of T, since (by our choice of reference) it involves no change in the number of liquid atoms. Thus, there is only one unknown parameter in the model,  $\Delta\Gamma_s$  (**Equation 1**)

We find we can reproduce the experimental results (**Figures 2c** and **S3**) to within their error bars by an appropriate choice of  $\Delta\Gamma_s$ . In particular, the calculated slope matches the measured one with no adjustable parameters, since to a good approximation changing  $\Delta\Gamma_s$  simply shifts the boundary up and down in temperature. The best fit with the experimental data is obtained for  $\Delta\Gamma_s = -0.037 \text{ J/m}^2$ . This is a tiny value, only 7% of the surface tension of Au-Si,<sup>[14]</sup> the key being simply that it is negative, rather than positive as in other systems. Thus, the existence of the surface phase can be explained simply by the solid phase having an unusually low surface energy, relative to the liquid. The model directly explains the surprisingly large range of stability observed: because the solid phase is Si-rich, its free energy decreases as the liquid becomes more Si-rich, stabilizing the phase to higher temperatures.

We find that the surface ordering plays a crucial role in the eutectic decomposition of liquid Au-Si into solid Au + solid Si on cooling. With experiments at high spatial and temporal resolution, we find that there are two steps in this process (**Figure S4**, **S5** and **Movie S3**). The liquid first solidifies into a metastable Au-Si crystalline phase, then this phase decomposes into crystalline Au and Si. Remarkably, the ordered surface layer appears unchanged throughout and the metastable phase grows from the ordered surface layer inward, and inherits the orientation of the surface phase (**Figure S5**). It is interesting that the surface phase survives even after the system decomposes into solid Au + Si (**Figure S6**).

Various metastable Au-Si phases are known to form as intermediate states during rapid quenching of Au-Si liquid.<sup>[15,12]</sup> The metastable phase observed in **Figure S5** is consistent with one of these phases,  $\delta_1$  (**Supporting Information**). We suggest that its good match with the

surface phase can explain why  $\delta_1$ , out of the many known metastable Au-Si solid phases,<sup>[16,12]</sup> is preferentially observed during cooling of nanoscale droplets where surface effects are dominant, while other metastable phases are more commonly found at the macroscale.<sup>[17]</sup> Our nanoscale droplets can be considerably supercooled (as in Figure 1a), indicating a substantial energy barrier to forming a solid.<sup>[18]</sup> When crystallization does take place, we see it starting at the surface. The ordered surface phase appears to act as a template for  $\delta_1$ , making this the crystallization pathway with lowest free energy barrier. In fact, we can consider the surface phase as a surface reconstruction of the  $\delta_1$  phase, as it persists at the surface of  $\delta_1$  after solidification.

We next consider how the surface ordering affects the catalytic properties of liquid Au-Si. Au-Si droplets are the first and most widely used catalysts for nanowire growth.<sup>[19,20]</sup> On supplying Si to a Au-Si droplet, the liquid becomes supersaturated with Si which then precipitates at the droplet/substrate interface to form a nanowire. In **Figure 3**, we show that the presence of surface ordering radically changes the ability of the droplet to catalyze this growth process. At constant Si flux (controlled via disilane pressure), nanowire growth decreases abruptly as the temperature is lowered. The dramatic change in growth rate correlates with formation of the surface phase (Figure 3b, 3c and Movie S4). The nanowire growth stops within our measurement capability, although we do not exclude the possibility that the wire is still growing at a very low rate, since slow growth has been observed near  $T_E$ <sup>[21]</sup> under conditions where the rate at higher temperature is 30x our value.

This connection between growth rate and surface ordering solves the longstanding puzzle of why Si nanowires cannot be grown below the eutectic temperature, while Ge and alloy Si-Ge nanowires can grow far below  $T_E$  from the supercooled liquid.<sup>[22,23,24]</sup> For Si, the catalytic activity of the liquid surface is quenched when the ordering appears. The behavior is consistent with observations that liquid surfaces are generally more reactive than crystalline surfaces in

catalysis of gases<sup>[25]</sup>, and also that nanowire growth from completely solid catalysts such as solid Au<sup>[26]</sup> or AuAg<sup>[27]</sup> is very slow compared with liquid catalysts. Nanowire growth involves several steps: sticking and dissociation at the catalyst surface, diffusion through the catalyst and addition of crystal layers at the liquid/nanowire interface. The present observation implies that the liquid surface has either a higher sticking probability or a higher efficiency in dissociating the precursor molecules than the ordered surface. From the present data we can not separate these two causes. However, we expect that the state of the interior of the catalyst (i.e. solid or liquid) is not likely to play a role since diffusion through either solid or liquid is not rate-limiting in nanowire growth.<sup>[28]</sup> In contrast to Au-Si, Au-Ge does not form a crystalline surface phase<sup>[29]</sup>, so its catalytic properties should be preserved at lower temperatures. Low temperature is in fact helpful for Ge nanowire growth as the morphology is improved by reduced sidewall deposition.<sup>[27,30,31]</sup>

To test the relationship between surface ordering and catalytic properties, we examined catalysis by droplets exposed to Si and Ge at constant temperature. In Figure 3d and Movie S5, we show that the ordered surface phase disappears after adding about one monolayer or less of Ge to the droplet, allowing growth below  $T_E$ . Ge and AuGe have lower surface energy than Si and AuSi respectively, so we expect Ge to segregate to the surface. Because our model shows that the stability of the Au-Si ordered phase is caused by its slightly lower surface energy compared to the liquid phase, even a small reduction in surface energy by Ge would be sufficient to destabilize it. On reintroducing pure Si<sub>2</sub>H<sub>6</sub>, the surface phase eventually reappears and growth stops (see Supporting Information). This suggests a strategy for sub- $T_E$  growth of nearly pure Si nanowires, which is to add a tiny fraction of Ge precursor to the Si source gas (see Supporting Information). A trace amount of Ge would be incorporated in the nanowire, but most properties would not be noticeably affected. Accessing low temperature would improve aspects of Si nanowire growth such as the sharpness of axial p/n junctions by reducing the solubility of dopants in the droplet. Indeed, the surface phase can be considered as a growth

tool: for example, changing the source gas conditions to create surface ordering would allow growth to be stopped without changing the pressure, which is known to destabilize droplets.<sup>[32]</sup>

The existence of the ordered surface phase on Au-Si over a range of conditions, and its role in the eutectic solidification pathway and effect on catalytic properties for Si nanowire growth, form a striking example of the unexpected phenomena that can occur at the surfaces of liquid metals. Liquid metals are well studied materials, yet there remain basic properties of their surfaces that can only be probed by controlled environment microscopy with good temporal and spatial resolution. The recent emergence of liquid metals as a new class of catalysts for the synthesis of graphene and other 2D materials<sup>[33]</sup> and 2D oxides<sup>[34]</sup> and for the catalytic conversion of gases<sup>[25]</sup> suggests that the study of surface phenomena in other liquid metals will be important in developing a deeper understanding and control of the properties of these materials.

## Experimental Section

### *Sample preparation and imaging*

We observed the formation of Au-Si surface phases *in situ* and with time resolution using two electron microscopes with complementary capabilities.

(1) A Hitachi H-9000 ultra-high vacuum TEM (UHV-TEM) was used to form Au-Si eutectic droplets and measure their surface structure and catalytic properties in the absence of effects due to background species in the microscope environment (water, oxygen). The instrument base pressure is  $2 \times 10^{-10}$  Torr and the maximum pressure during imaging is  $2 \times 10^{-5}$  Torr. This microscope is connected to a cluster of UHV tools where metal deposition was carried out. The substrates used were  $3 \text{ mm} \times 300 \text{ }\mu\text{m}$  silicon strips cut from a  $700 \text{ }\mu\text{m}$  thick (111) wafer. Each sample was loaded to the TEM loadlock, where it was baked at  $100 - 150 \text{ }^\circ\text{C}$  under a tungsten lamp for 8h to degas and remove moisture. It was then transferred to a UHV

chamber and heated resistively by direct current up to 1200 °C for short pulses in order to desorb the native oxide and form flat Si terraces. At the same time, a temperature vs. heating current curve was measured by using a pyrometer to observe the sample through a viewport. The sample was then transferred under vacuum to a Knudsen cell Au evaporation system, thus maintaining an oxide-free surface. About 1 nm Au was deposited onto the {111} surface to act as the VLS catalyst. The sample was finally transferred under vacuum to the TEM where precursor gas ( $\text{Si}_2\text{H}_6$ ) was introduced through a capillary tube and the temperature was raised to 500 °C, again using direct current heating. This agglomerates Au into droplets and initiates VLS growth. Typical growth rates are in the range 5-15 nm/min at temperatures of 470-520 °C. The presence of the surface ordering (visible as facets on otherwise amorphous droplets) and the nanowire growth rate as a function of temperature were accurately determined from such *in situ* observations. For accurate temperature measurement, the temperature vs. heating current curve was calibrated by identifying the current flowing at the eutectic phase transformation, using slow ramping upwards through the eutectic transformation.

(2) An aberration corrected FEI Titan 300 environmental TEM (ETEM) with capabilities to introduce group IV gas precursors and also equipped with a Gatan K2 fast camera (400 images per second) was used to provide high spatial and temporal resolution of structural changes of the Au-Si surface and bulk phases. Samples on which nanowires had been pre-grown in the UHV-TEM were carried through air then loaded into the ETEM. A shell of  $\text{SiO}_2$  was visible around the nanowires but this could be removed by condensing the intense electron beam spot around the catalyst droplet while holding the sample at 500 °C. Growth of wires and formation and destruction of surface ordering were obtained by flowing  $\text{Si}_2\text{H}_6$  and  $\text{Ge}_2\text{H}_6$ . Separately, isothermal experiments were performed on Au aerosol particles on nitride-coated Si samples (3 mm  $\times$  300  $\mu\text{m}$  silicon strips cut from a 700  $\mu\text{m}$  thick (111) wafer). For these samples, 5 and 10 nm Au aerosol nanoparticles were deposited directly on the nitride layer. Sample were mounted

in a conventional heating holder (Gatan) and imaged with the nitride-coated surface parallel to the beam. This heating holder uses current flow through a furnace surrounding the sample, measuring temperature via a thermocouple attached to the furnace. We checked that the solid-liquid transition happened at the same temperature in the UHVTEM calibrated with the pyrometer and in the ETEM as indicated by the thermocouple. The maximum gas pressures used are low ( $2 \times 10^{-5}$  Torr) and do not affect the substrate temperature. Any cooling effect due to the introduction of the gas would result in a drift of the sample, which we did not observe. Cooling from the gas in ETEM is generally not visible below the  $1 \times 10^{-3}$  Torr range.

This allowed direct observation in the ETEM of formation of the surface phase while changing the Au-Si composition at a given temperature. Experiments were repeated to verify that the formation of the surface phase occurred at the same temperature and composition over a large sample substrate. In particular, we verified that there was no visible difference between particles constantly exposed to the electron beam and particles observed sporadically. Images were recorded using a Gatan K2-IS camera acquiring 400 images per second each having 4 mega-pixels.

#### *Model for thermodynamics of surface ordering*

The  $N$  values used in the model are taken from Ref 2,  $N_{Au} = 9.6 \times 10^{-6}$  and  $N_{Si} = 19.2 \times 10^{-6}$  mol/m<sup>2</sup> for one monolayer. Since our observations and Ref (8) show that the surface phase actually contains two monolayers, we doubled these values for our calculations. It is important to note that doubling the  $N$  values does not change the fitted curve, it simply doubles the value of the fitting parameter  $\Delta\Gamma_s$ . In particular, the slope of the curve is unaffected. Thus, the conclusions are the same whether we model a single or a double layer.

**Supporting Information:** Supporting Information is available from the Wiley Online Library or from the author.

**Competing interests:** Authors declare no competing interests.

**Data and materials availability:** Raw data is available upon request to the corresponding authors.

**Acknowledgments:** The authors acknowledge Arthur Ellis for technical support, Dominique Chatain for helpful and stimulating discussion and Daniel Jacobsson for Au particle deposition.

**Funding:** ERC Grant 279342: InSituNANO and EPSRC (Grants: EP/K016636/1, EP/P005152/1) (F.P., S.H.). The Center for Functional Nanomaterials, Brookhaven National Laboratory, which is supported by the U.S. Department of Energy, Office of Basic Energy Sciences, under contract DE-AC02-98CH10886 (A.D.G, D.Z. and E.A.S.).

## References

- [1] A. Turchanin, W. Freyland, D. Nattland, *Physical Chemistry Chemical Physics*, **2002** 4(4), 647-654.
- [2] O. G. Shpyrko, R. Streitel, V. S. Balagurusamy, A.Y. Grigoriev, M. Deutsch, B. M. Ocko, M. Meron, B. Lin, P. S. Pershan, *Science*, **2006** 313, 77-80.
- [3] M. J. Regan, E. H. Kawamoto, S. Lee, Peter S. Pershan, N. Maskil, M. Deutsch, O. M. Magnussen, B. M. Ocko, L. E. Berman, *Physical review letters* **1995** 75, 2498.
- [4] O. M. Magnussen, B. M. Ocko, M. J. Regan, K. Penanen, Peter S. Pershan, M. Deutsch, *Physical review letters* **1995**, 74, 4444.
- [5] B. Yang, D. Gidalevitz, D. Li, Z. Huang, S. A. Rice, *Proceedings of the National Academy of Sciences*, **1999**, 96(23), 13009.
- [6] C. Calmes, D. Giuranno, D. Chatain, *Journal of materials science*, **2009**, 44(22), 5949.
- [7] B. Yang, D. Li, S. A. Rice, *Physical Review B*, **2003**, 67(21), 212103.
- [8] S. Mechler, P.S. Pershan, E. Yahel, S. E. Stoltz, O. G. Shpyrko, B. Lin, M. Meron, S. Sellner, *Physical review letters*, **2010**, 105(18), 186101.

- [9] O. G. Shpyrko, R. Streitel, V. S. Balagurusamy, A. Y. Grigoriev, M. Deutsch, B. M. Ocko, M. Meron, B. Lin, P. S. Pershan, *Physical Review B*, **2007**, 76(24), 245436.
- [10] A. L. Pinaridi, S. J. Leake, R. Felici, I. K. Robinson, *Physical Review B*, **2009**, 79(4), 045416.
- [11] B. Pluis, D. Frenkel, J. F. Van der Veen, *Surface science*, **1990**, 239(3), 282.
- [12] H. Okamoto, T. B. Massalski, *Bulletin of Alloy Phase Diagrams*, **1983**, 4, 190.
- [13] P. Y. Chevalier, *Thermochimica Acta*, **1989**, 141, 217-226.
- [14] F. Panciera, M. M. Norton, S. B. Alam, S. Hofmann, K. Mølhave, F. M. Ross, *Nature Communications*, **2016**, 7.
- [15] M. Zhang, J. G. Wen, M. Y. Efremov, E. A. Olson, Z. S. Zhang, L. Hu, L. P. de la Rama, R. Kumamuru, K. L. Kavanagh, Z. Ma, L. H. Allen, *Journal of Applied Physics*, **2012**, 111(9), 093516.
- [16] L. Hultman, A. Robertsson, H. T. G. Hentzell, I. Engström, P. A. Psaras, *Journal of Applied Physics*, **1987**, 62(9), 3647.
- [17] H. S. Chen, D. Turnbull, *Journal of Applied Physics*, **1967**, 38(9), 3646.
- [18] T. U. Schüllli, R. Daudin, G. Renaud, A. Vaysset, O. Geaymond, A. Pasturel, *Nature*, **2012**, 464(7292), 1174.
- [19] R. S. Wagner, W. C. Ellis, *Appl. Phys. Lett.* **1964**, 4, 89.
- [20] V. Schmidt, J. V. Wittemann, U. Gosele, *Chemical reviews*, **2010**, 110(1), 361.
- [21] C. W. Pinion, D. J. Hill, J. D. Christesen, J. R. McBride, J. F. Cahoon, Barrierless, *The Journal of Physical Chemistry Letters*, **2016**, 7(20), 4236.
- [22] S. A. Dayeh, J. Wang, N. Li, J. Y. Huang, A. V. Gin, S. T. Picraux, *Nano letters*, **2011**, 11(10), 4200.
- [23] K. K. Lew, L. Pan, E. C. Dickey, J. M. Redwing, *Advanced Materials*, **2003**, 15(24), 2073.

- [24] K. K. Lew, L. Pan, E. C. Dickey, J. M. Redwing, *Journal of materials research*, **2006**, 21(11), 2876.
- [25] N. Taccardi, M. Grabau, J. Debuschewitz, M. Distaso, M. Brandl, R. Hock, F. Maier, C. Papp, J. Erhard, C. Neiss, W. Peukert, *Nature chemistry*, 9(9), **2017**, 862.
- [26] S. R. Kodambaka, J. Tersoff, M. C. Reuter, F. M. Ross, *Science*, **2007**, 316, 729.
- [27] Y. C. Chou, C. Y. Wen, M. C. Reuter, D. Su, E. A. Stach, F. M. Ross, *ACS nano*. **2012**, 6(7), 6407.
- [28] A. I. Persson, M.W. Larsson, S. Stenström, B.J. Ohlsson, L. Samuelson, L.R. Wallenberg, *Nature materials*, **2004**, 3(10), 677.
- [29] P. S. Pershan, S. E. Stoltz, S. Mechler, O. G. Shpyrko, A. Y. Grigoriev, V. S. K. Balagurusamy, B. H. Lin, M. Meron, *Physical Review B*, **2009** 80(12), 125414.
- [30] H. Adhikari, P. C. McIntyre, A. F. Marshall, C. E. Chidsey, *Journal of Applied Physics*, **2007**, 102(9), 094311.
- [31] A. D. Gamalski, J. Tersoff, R. Sharma, C. Ducati, S. Hofmann, *Nano letters*, **2010**, 10(8), 2972.
- [32] B. Tian, P. Xie, T. J. Kempa, D. C. Bell, C. M. Lieber, *Nature nanotechnology*, **2009**, 4(12), 824.
- [33] S. Y. Li, C. Lin, W. Zhao, J. Wu, Z. Wang, Z. Hu, Y. Shen, D. M. Tang, J. Wang, Q. Zhang, H. Zhu, L. Chu, W. Zhao, C. Liu, Z. Sun, T. Taniguchi, M. Osada, W. Chen, Q. H. Xu, A. T. S. Wee, K. Suenaga, F. Ding, G. Eda, *Nature Materials*, **2018**, 17, 535.
- [34] A. Zavabeti, J. Z. Ou, B. J. Carey, N. Syed, R. Orrell-Trigg, E. L. Mayes, C. Xu, O. Kavehei, A. P. O'Mullane, R. B. Kaner, K. Kalantar-zadeh, *Science*, **2017**, 358(6361), 332.
- [35] S. Kodambaka, J. Tersoff, M. C. Reuter, F. M. Ross, *Physical Review Letters*, **2006**, 96(9), 096105.

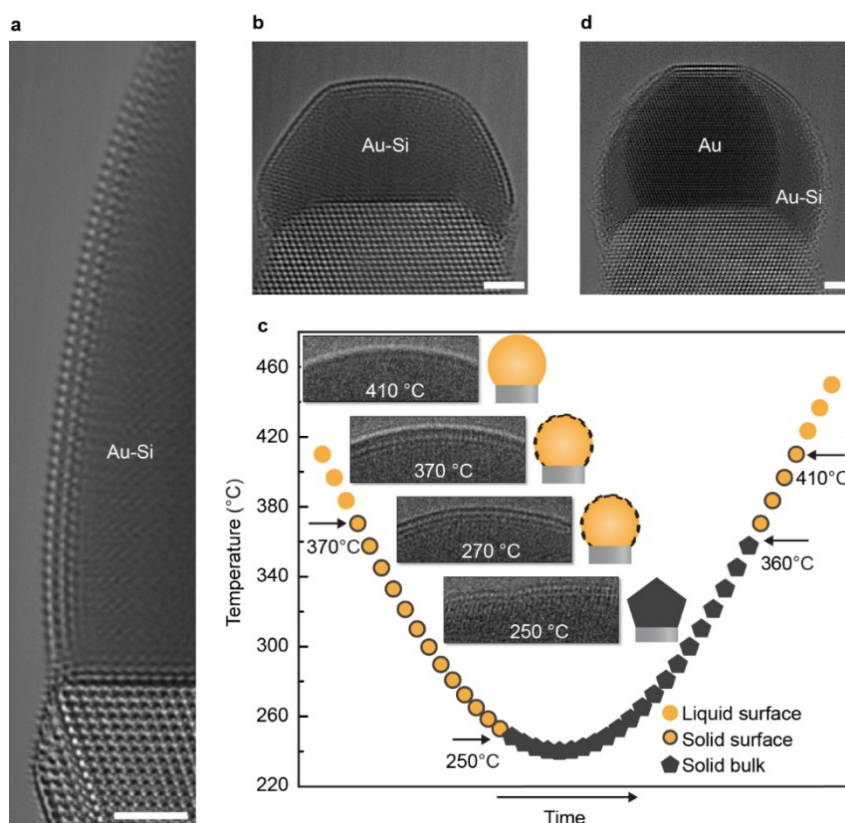


**Figure 1.** Crystalline ordering at the surface of Au-Si liquid. a) The 2D surface phase on a 50 nm diameter droplet at 350 °C using aberration corrected microscopy with sub-images aligned to remove effects of drift. A crystalline bilayer is visible with interlayer spacing 0.35 nm (Table S1). The contrast visible over the entire liquid droplet is assumed to be a projection of ordering present on top and bottom surfaces. b) Surface ordering on a smaller 12 nm diameter droplet at 350 °C. Several 2D domains are visible separated by high-curvature boundaries. Thermal motion of the structure is shown in Supplementary Movie S1. c) Schematic summary of the evolution during cooling and heating, with insets showing one particular droplet during cooling. d) Image obtained during heating of a solid Au particle on Si. At the time shown,  $T = 360$  °C and the Au has partially reacted with Si so that eutectic liquid covers part of its surface. Ordering is visible both on the liquid surface and on the (111) surface of the remaining solid Au. All scale bars are 2 nm.

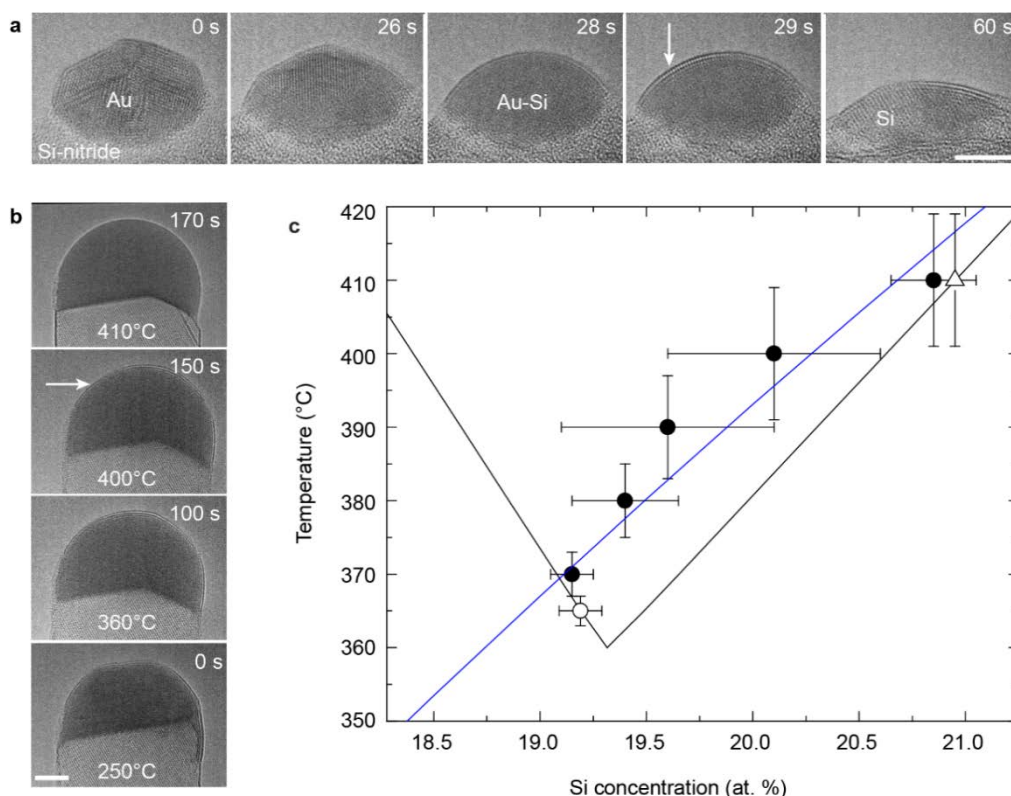


**Figure 2.** Surface ordered phase vs temperature and composition of liquid Au-Si. Solid arrows indicate the formation of the ordered 2D phase. All scale bars are 5 nm. a) Au nanoparticles on SiN exposed to  $\text{Si}_2\text{H}_6$  ( $1.5 \times 10^{-5}$  Torr) at 370 °C. The ordered phase appears just after complete reaction of solid Au. b) Si nanowire heated in vacuum. The solid to liquid Au-Si transition and the 2D phase appear at 360 °C (i.e. the expected eutectic temperature); the 2D phase disappears at 410 °C. c) Au-Si phase diagram near the eutectic point. Solid circles, from the complete data set in Figure S2, show the liquid composition at which the 2D phase appears during isothermal addition of Si. Open circle shows the temperature at which the 2D phase is already visible as soon as liquid appears, indicating that this point lies below the phase boundary. Open triangle shows disappearance of order during heating in equilibrium with Si. The blue line shows the calculated phase boundary for the melt/freeze transition of the solid surface layer using a value of  $\Delta\Gamma_s = -0.037 \text{ J/m}^2$  obtained by fitting to the solid circle data points.

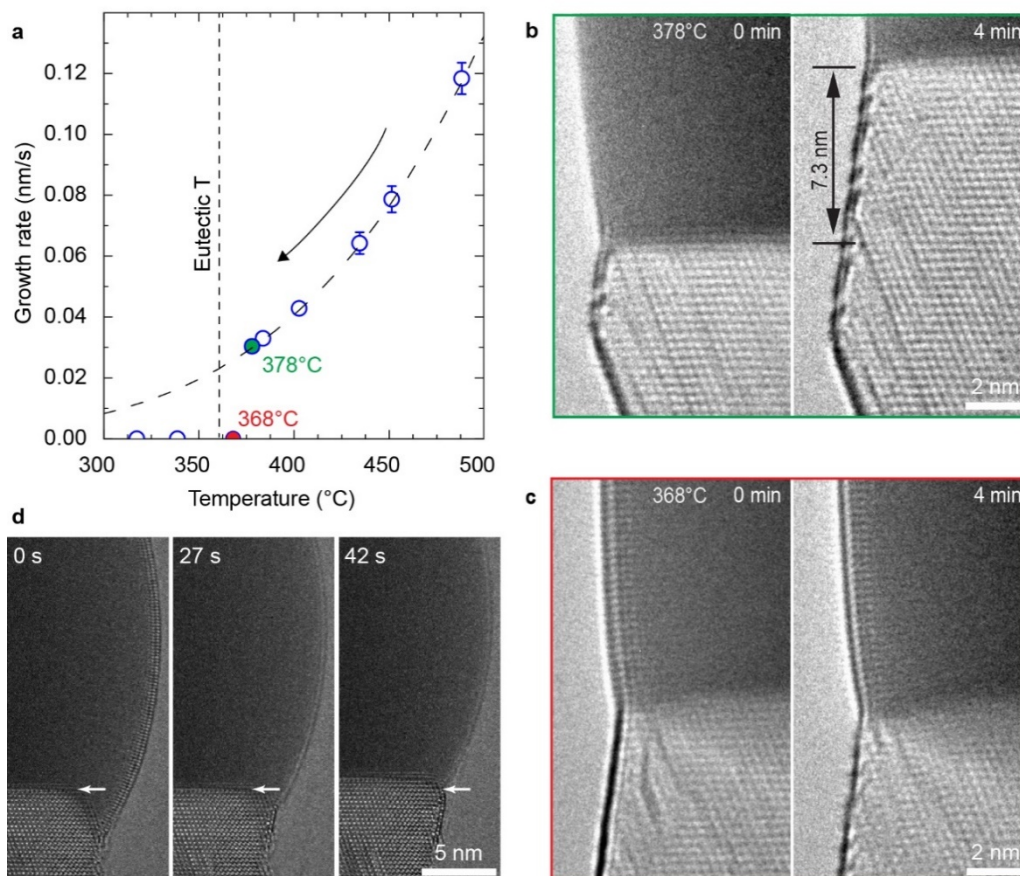


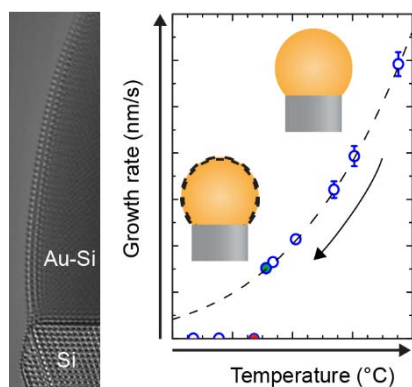
**Figure 3.** Impact of the surface phase on catalytic properties. a) Growth rate vs temperature during cooling, for a Si nanowire growing in  $1 \times 10^{-5}$  Torr  $\text{Si}_2\text{H}_6$ . The error in T is  $\pm 10$  °C. The error bar on the growth rate is calculated assuming uncertainties in measurement of length 1 nm and time 0.05 s. For each temperature, growth of a segment of  $\sim 15$  nm was timed; lower T required more time, giving smaller error. The growth rate decreases smoothly with decreasing T, as expected,<sup>[35]</sup> until a break at  $\sim 375$  °C below which no measurable growth was observed after 45 min. b) Images at 378 °C at the times indicated, showing growth (at  $0.03 \text{ nm s}^{-1}$ ) and no order at the droplet surface. Data corresponds to the green circle in A. c) Images at 368 °C showing no growth and the presence of the surface ordered layer. Data corresponds to the red circle in A. The full data set is shown in Supplementary Movie S4. d) Images recorded at 350 °C showing ordered surface in the absence of precursor gases; ordering disappears after 27 s exposure to  $2 \times 10^{-5}$  Torr  $\text{Ge}_2\text{H}_6$ ; after 42 s, growth restarted to form a segment of SiGe (arrowed).

**In situ transmission electron microscopy reveals the presence of an atomically thin crystalline phase at the surface of liquid Au-Si.** This surface ordering plays a key role in the pathway by which the Au-Si eutectic solidifies and also dramatically affects the catalytic properties of the liquid, explaining the anomalously slow growth kinetics of Si nanowires at low temperature.

Keywords: (surface freezing, nanowires, *in situ* transmission electron microscopy, 2D crystals, metastable phases)

*Federico Panciera,\* Jerry Tersoff, Andrew D. Gamalski, Mark C. Reuter, Dmitri Zakharov, Eric A. Stach, Stephan Hofmann, Frances M. Ross\**

### Surface crystallization of liquid Au-Si and its impact on catalysis



## Supporting Information

### Surface crystallization of liquid Au-Si and its impact on catalysis

*Federico Panciera,\* Jerry Tersoff, Andrew D. Gamalski, Mark C. Reuter, Dmitri Zakharov, Eric A. Stach, Stephan Hofmann, Frances M. Ross\**

#### Table of contents:

Supplementary Text .....	19
Supplementary Tables .....	21
Supplementary Figures.....	22
Supplementary Movie Captions .....	26
Supplementary References .....	28

#### Supplementary Text

##### Effect of Ge on the surface phase

We test the effect of Ge on the Au-Si surface phase by first growing Si from an Au-Si droplet at higher temperature. On cooling to 350 °C, surface ordering appears and the growth rate decreases to an unmeasurably small value. We then deliver Ge to the droplet by switching gas precursors from Si<sub>2</sub>H<sub>6</sub> to Ge<sub>2</sub>H<sub>6</sub>. After ~ 27 s at 2×10<sup>-5</sup> Torr Ge<sub>2</sub>H<sub>6</sub>, the surface phase disappears (Movie S5). When Si is again supplied, growth restarts but only until the surface phase reappears after ~7 min. It is possible to create and destroy the surface phase repeatedly: surface ordering consistently disappears after ~30 s exposure to Ge<sub>2</sub>H<sub>6</sub> and reappears after ~7 min exposure to Si<sub>2</sub>H<sub>6</sub>.

The faster effect of Ge is presumably due to the segregation of the supplied Ge at the droplet surface. We expect segregation because Ge and Au-Ge have lower surface energy than Si and Au-Si respectively.<sup>[36]</sup> This Ge-rich layer would replace the Au-Si layer and disrupt the crystalline phase. We calculate, approximately, that less than 1 ML of Ge is sufficient to destroy the surface ordering, as follows: The growth rate after ordering disappears is 0.043 nm/s, or ~

4 ML per 30 s. The droplet surface is about 3 times larger than the wire cross-section. Thus in the 30 s required for the ordering to disappear, we add a maximum of 1.3 ML of Ge at the droplet surface. Here, we assume that the Ge incorporation rate is the same with and without the 2D surface phase. Since it is likely that the 2D phase impedes the incorporation of Ge (as it does for Si) the amount of Ge incorporated would be less than 1 ML. On reintroducing disilane, the time for the surface phase to reappear is then longer (7 min) In this time, the single ML (or less) of Ge at the droplet surface might be incorporated into the nanowire or evaporated to leave a surface concentration that is too low to prevent crystallization.

The stability of the ordered surface phase may be controllable through other surface reactions. Intriguingly, Si nanowire growth rates can be preserved below  $T_E$  by adding HCl to the source gas.<sup>[21]</sup> We interpret this observation as a clue that the gas environment can control the presence of surface ordering and therefore growth kinetics.

The introduction of any gas to promote the growth of Si NWs below the eutectic temperature could result in the incorporation of impurities inside the NWs. Here we estimate the amount of Ge that would be introduced using the experimental conditions used in our experiment: 350 °C,  $2 \times 10^{-5}$  Torr  $\text{Ge}_2\text{H}_6$ . In 7 min, we expect 28 ML Si to grow. If all the Ge at the surface were incorporated in the crystal, it would correspond to 4 ML Ge. Thus, the crystal composition could be as high as  $4/28=15\%$ . However, this is an overestimate because the amount of Ge in the droplet corresponds to growth of the nanowire by less than 4ML, and some of this is presumably still present at the surface when crystallization occurs. Moreover, this represents the average over the 7 minute period. The concentration of Ge in the liquid must be decreasing during this time (in equilibrium with the surface depletion), and the concentration near the end of the 7 min represents the minimum needed to maintain a liquid surface. Thus in practice, using the smallest amount of Ge that is sufficient to maintain a liquid surface would result in a wire composed of Si with at most a few percent of Ge, not enough to appreciably affect most properties.

## Supplementary Tables

**Supplementary Table 1. Structure and composition of surface and bulk metastable phases observed in Au-Si.** Published parameters compared with current observations. While we have no direct measurement of composition, we assume the observed surface ordered phase is the LT phase as they are found under similar conditions and share two lattice parameters. Similarly, we assume the observed metastable bulk phase is the Au-Si  $\delta_1$  phase since measured parameters  $b$  and  $c$  are similar to an in-plane spacing and the out-of-plane spacing of  $\delta_1$ .

Author, name of the phase, (References)	Temperature at which phase is observed	Largest in- plane parameter Å	Smallest in- plane param. Å	Parameter perpendicular to surface or thickness Å	Composition	Comments
<b>Surface phases</b>						
Green <sup>[37]</sup>	RT	9.35	7.35	30Å thick at 250 °C		LEED
Green <sup>[38]</sup>	RT	9.33	7.35	6.80		
Shpyrko, LT phase <sup>[7,8,9]</sup>	363- 371 °C	9.39	7.39	2ML thick	Au <sub>4</sub> Si <sub>8</sub>	XRD and XRR
Shpyrko, HT A phase <sup>[9]</sup>	371-432 °C	5.41	4.25	1ML thick	Au <sub>4</sub> Si <sub>2</sub>	XRD and XRR
Shpyrko, HT B phase <sup>[9]</sup>	371-432 °C	3.66	2.94	1ML thick	AuSi <sub>2</sub>	XRD and XRR
This study	363-410 °C	2.2 (Supp. Fig. 1b), 3.4 (Supp. Fig. 5a) (combination of a and b; depend on orientation)	7.3 (Fig. 3a)	2ML thick 3.5 (Supp. Fig. 5a)		
<b>Bulk phases</b>						
Gaigher <sup>[39]</sup>	RT	9.56	7.5	6.8		From thick crystals
Baumann <sup>[40]</sup>	RT	9.71	7.68	7.03		Au silicides precipitates in Si
Zhang <sup>[15]</sup>	RT	9.2	7.2	6.75	Au <sub>0.74</sub> Si <sub>0.26</sub>	TEM diffr. and EDS
This study	250 °C		7.31 (Fig. 3a)	6.56 for paired layers, 2 × 3.28 (Fig. 3a)		

## Supplementary Figures

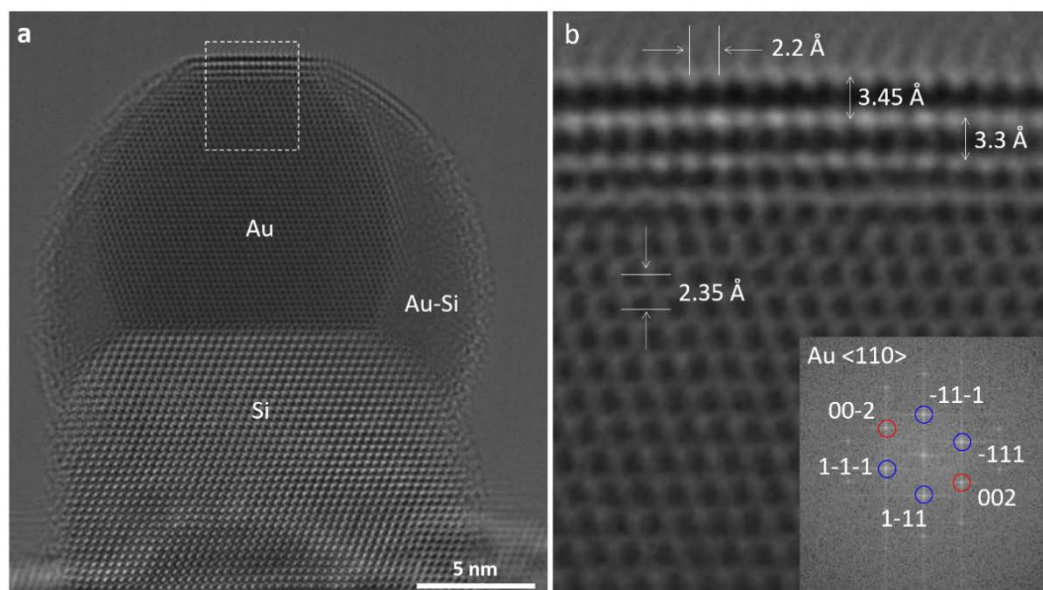


**Figure S1. Surface ordered phase on solid Au.** A Si nanowire was grown at 450 °C then cooled to RT in order to fully crystallize the catalyst. a) During reheating to 360 °C we observe the coexistence of solid FCC Au, liquid Au-Si and the surface ordered phase both on solid and liquid. Si and Au are viewed along the  $\langle 110 \rangle$  direction and exhibit an epitaxial interface. b) Enlargement of the box in (a) showing the atomic structure of the surface phase and its interface with Au.

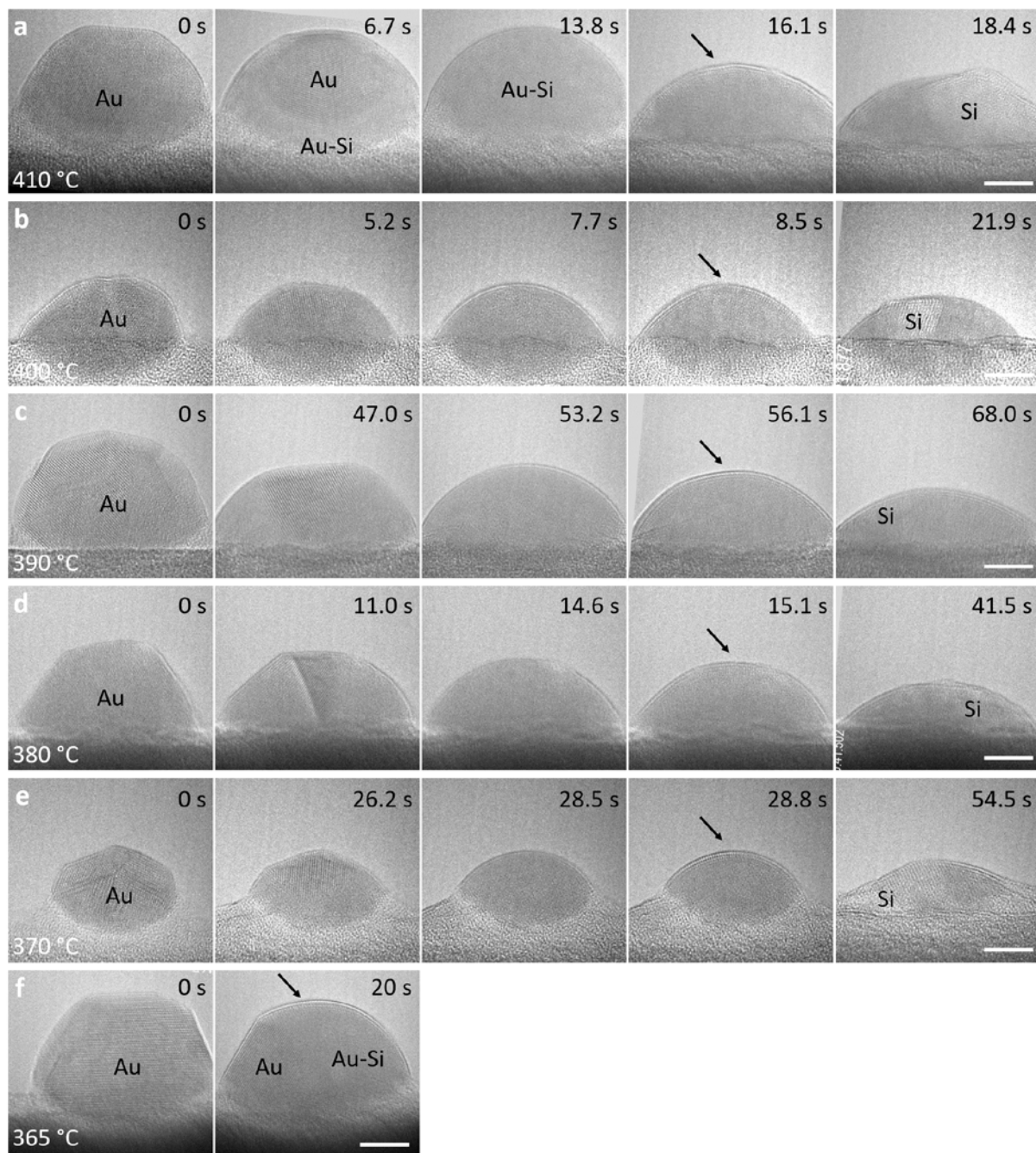


**Figure S2. Surface ordered phase vs temperature and composition of liquid Au-Si.** Aerosol Au nanoparticles deposited on a SiN substrate and exposed to  $1.5 \times 10^{-5}$  Torr  $\text{Si}_2\text{H}_6$  at different temperatures. All scale bars are 5 nm. a) At 410 °C the ordered phase appears just before Si nucleation. b-e) At lower temperatures, the phase appears progressively closer to the Au liquidus line. (Panel (e) is also shown in Figure 2a.) f) At 365 °C the phase appears when Au is still partially solid. Arrows indicate the first visible image of the ordered phase.

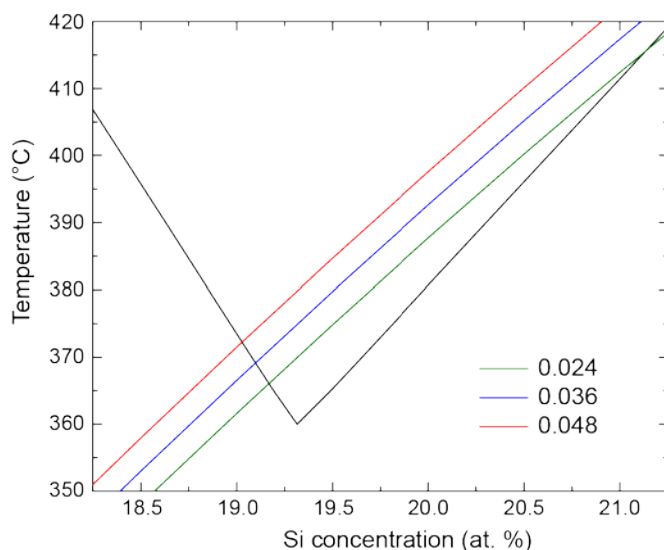


**Figure S3. Optimization of the fitting parameter.** The calculated Au and Si liquidus lines which define the bulk phase diagram are shown in black. The colored lines show the transition between a normal liquid surface and a solid surface layer, for three different values of the unknown parameter:  $\Delta\Gamma_s = -0.024$ ,  $-0.036$ , and  $-0.048$  J/m<sup>2</sup> when referenced to the elemental solids.

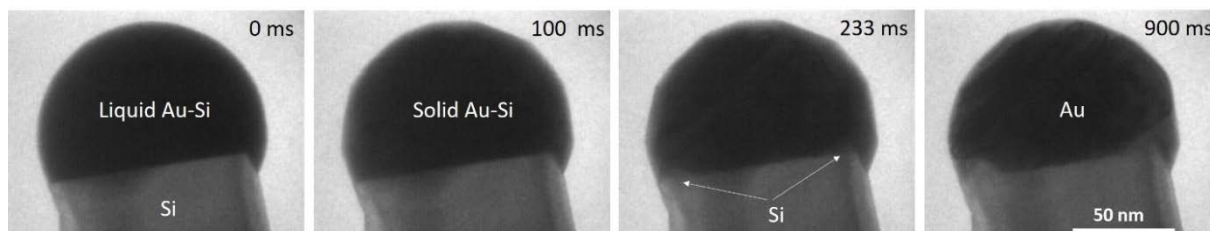


**Figure S4. Crystallization of Au-Si eutectic alloy at 250 °C.** Sequence of images recorded in UHV TEM during cooling of Au catalyzed Si nanowire in vacuum. The crystallization happens in two steps: first, the liquid Au-Si solidifies in a metastable phase having the same composition as the liquid; second, the metastable phase undergoes a phase separation into pure Au and Si.

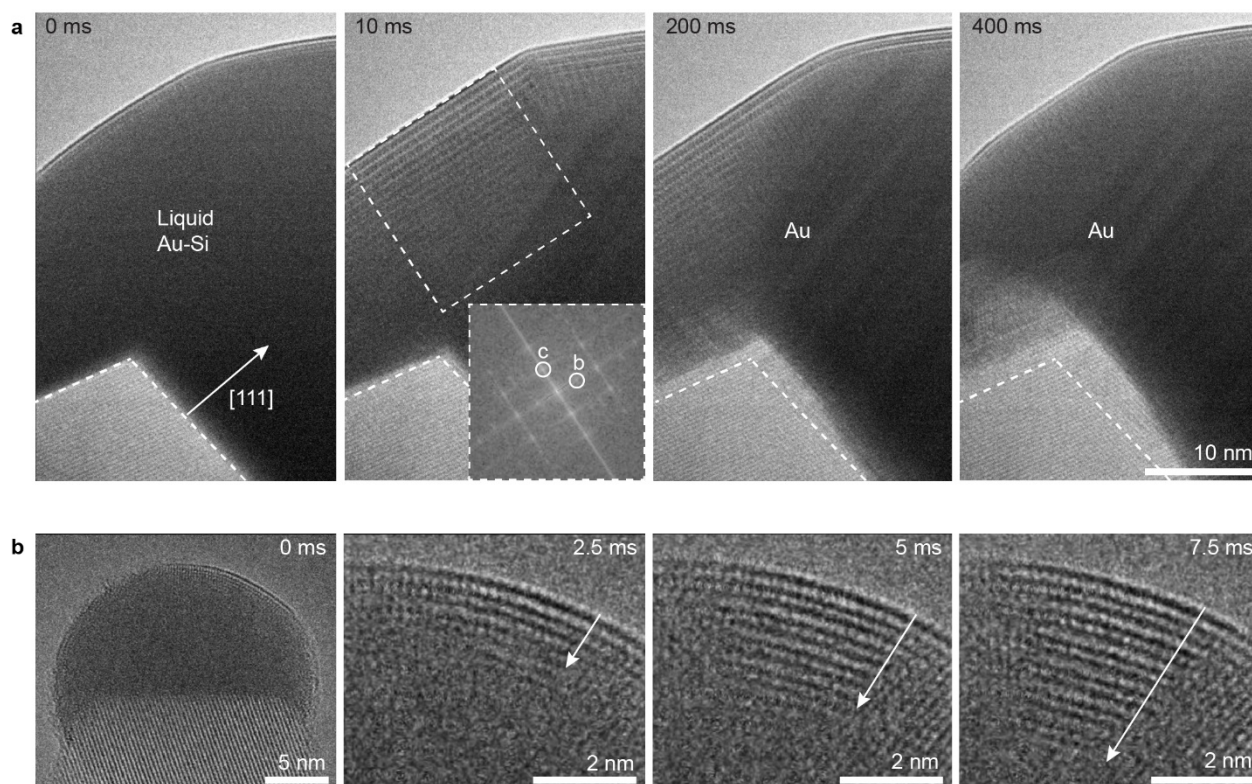


**Figure S5. Solidification of liquid Au-Si.** a) Sequence of images showing the two-step solidification process of liquid Au-Si on cooling through 250 °C. Initially surface ordering is present. Within 10 ms, a metastable phase forms with ordering shown in the inset FFT and summarized in Table S1. After 400 ms, this separates into Au and Si: the Si is added at the Si interface. b) Sequence of images recorded at 400 fps showing the details of the metastable phase formation starting from the surface phase and growing inward. In this droplet, formation of the metastable phase is complete at 7.5 msec.

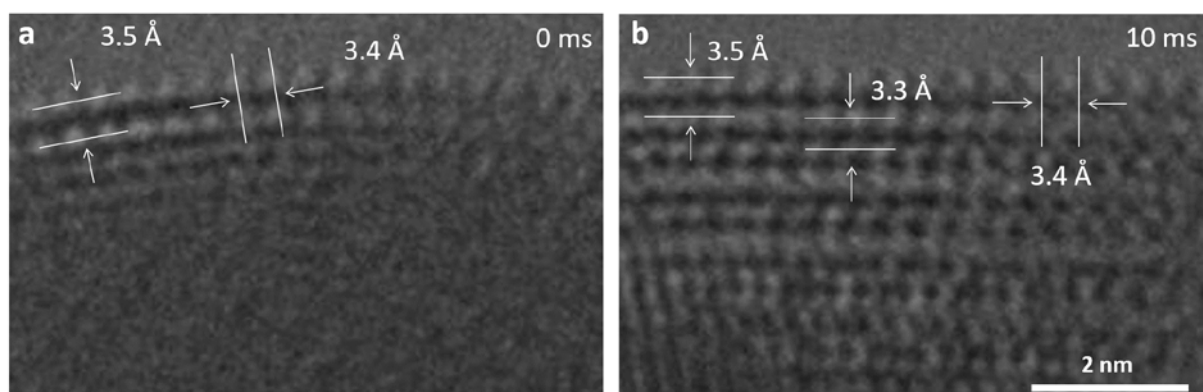
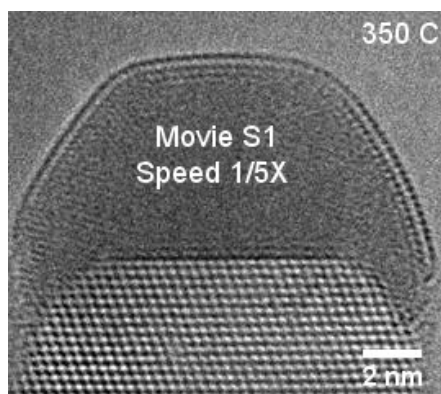


**Figure S6. Atomic structure of the surface and metastable phases.** Enlarged images of a region of an Au-Si surface at 250 °C, immediately before (a) and after solidification (b). The initial two monolayers with identical in-plane order remain while the newly formed layers have the same lateral spacing but smaller vertical spacing (0.33nm), which is the same as in Figure S5.

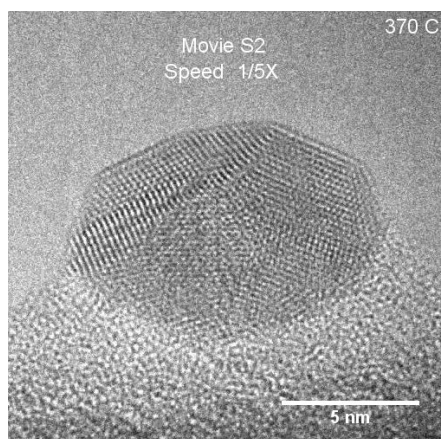
## Supplementary Movie Captions

## Movie S1



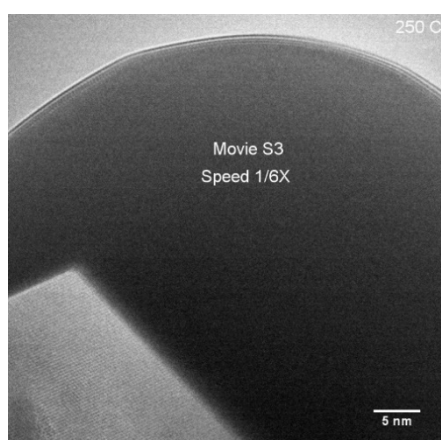
**2D crystalline surface phase on a liquid Au-Si droplet.** The 2D Au surface phase is visible on the surface of liquid Au-Si at 350 °C in vacuum. It is composed of different domains and the domain boundaries are mobile. Recorded at 400 fps, images are integrated 5 by 5. Image  $n'$  is the average of image  $n-2$ ,  $n-1$ ,  $n$ ,  $n+1$ ,  $n+2$ ; image  $n'+1$  is the average of  $n+3$ ,  $n+4$ ,  $n+5$ ,  $n+6$ ,  $n+7$  with  $n$  representing the  $n$ th image in the original video (400 fps) and  $n'$  representing the  $n$ th image of the edited video ( $n'=n/5$ ). Speed is reduced to 1/5 of the original.

## Movie S2

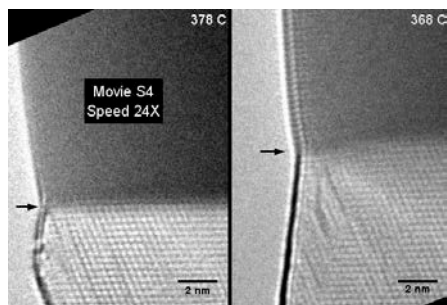


**Order appears when Au-Si liquid composition is changed.** A Au nanoparticle deposited on a SiN substrate is exposed to  $\text{Si}_2\text{H}_6$  ( $1.5 \times 10^{-5}$  Torr) at 370 °C. The Au nanoparticle ordered phase appears just after the complete dissolution of Au-Si. Recorded at 400 fps, images are integrated 5 by 5. Speed is reduced to 1/5 of the original.

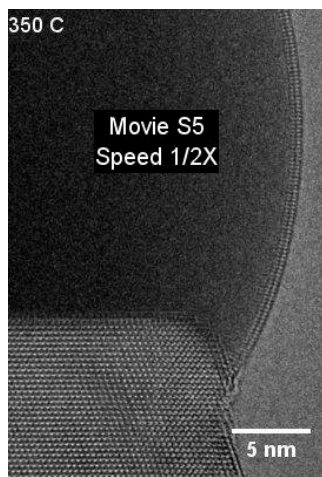
## Movie S3



**Solidification of the AuSi droplet.** Solidification process of liquid Au-Si on cooling through 250°C. Surface facets and ordering is present initially. Solidification of the interior liquid is visible followed by phase separation into Au and Si. Recorded at 400 fps, images are integrated 5 by 5. Speed is reduced to 1/5 of the original.

**Movie S4**

**Growth rate with and without order.** Videos of the same wire recorded at pressure of  $1 \times 10^{-5}$  Torr of  $\text{Si}_2\text{H}_6$  and temperature of  $378^\circ\text{C}$  (left) and  $368^\circ\text{C}$  (right), showing that the presence of the surface phase virtually arrests the wire growth. Video recorded at 4 fps. Speed is 24 times faster than the original.

**Movie S5**

**Surface order disappears when Ge is added.** Recorded at 400 fps, images are integrated 5 by 5. Speed is reduced to 1/2 of the original.

**Supplementary References**

- [36] Y. V. Naidich, V. M. Perevertailo, L. P. Obushchak. *Powder Metallurgy and Metal Ceramics*. **1975** 14(5), 403.
- [37] A. K. Green, E. Bauer, *Journal of Applied Physics*, **1976**, 47(4), 1284.
- [38] A. K. Green, E. Bauer, *Journal of Applied Physics*, **1981**, 52(8), 5098.
- [39] H. L. Gaigher, N. G. Berg, *Thin Solid Films*, **1980**, 68(2), 373.
- [40] F. H. Baumann, W. Schröter, *Physical Review B*, **1991**, 43(8), 6510.